Published in final edited form as:
Int J Hyperthermia. 2011 ; 27(2): 140–155. doi:10.3109/02656736.2010.528140.

Formulation and characterisation of magnetic resonance imageable thermally sensitive liposomes for use with magnetic resonance-guided high intensity focused ultrasound

AYELE H. NEGUSSIE[1,†], **PAVEL S. YARMOLENKO**[1,2,†], **ARI PARTANEN**[1,3], **ASHISH RANJAN**[1], **GENEVIEVE JACOBS**[1], **DAVID WOODS**[1], **HENRY BRYANT**[4], **DAVID THOMASSON**[5], **MARK W. DEWHIRST**[6], **BRADFORD J. WOOD**[1], and **MATTHEW R. DREHER**[1]

[1]Center for Interventional Oncology, Radiology and Imaging Sciences, Clinical Center, National Institutes of Health, Bethesda, Maryland [2]Department of Biomedical Engineering, Duke University, Durham, North Carolina [3]Philips Healthcare, Cleveland, Ohio [4]Laboratory of Diagnostic Radiology Research, Radiology and Imaging Sciences, Clinical Center, National Institutes of Health, Bethesda, Maryland [5]Radiology and Imaging Sciences, Clinical Center, National Institutes of Health, Bethesda, Maryland [6]Department of Radiation Oncology, Duke University, Durham, North Carolina, USA

Abstract

Purpose—Objectives of this study were to: 1) develop iLTSL, a low temperature sensitive liposome co-loaded with an MRI contrast agent (ProHance® Gd-HP-DO3A) and doxorubicin, 2) characterise doxorubicin and Gd-HP-DO3A release from iLTSL and 3) investigate the ability of magnetic resonance-guided high intensity focused ultrasound (MR-HIFU) to induce and monitor iLTSL content release in phantoms and *in vivo*.

Methods—iLTSL was passively loaded with Gd-HP-DO3A and actively loaded with doxorubicin. Doxorubicin and Gd-HP-DO3A release was quantified by fluorescence and spectroscopic techniques, respectively. Release with MR-HIFU was examined in tissue-mimicking phantoms containing iLTSL and in a VX2 rabbit tumour model.

Results—iLTSL demonstrated consistent size and doxorubicin release kinetics after storage at 4°C for 7 days. Release of doxorubicin and Gd-HP-DO3A from iLTSL was minimal at 37°C but fast when heated to 41.3°C. The magnitude of release was not significantly different between doxorubicin and Gd-HP-DO3A over 10 min in HEPES buffer and plasma at 37°, 40° and 41.3°C ($p>0.05$). Relaxivity of iLTSL increased significantly ($p<0.0001$) from 1.95 ± 0.05 to 4.01 ± 0.1 mMs^{-1} when heated above the transition temperature. Signal increase corresponded spatially and temporally to MR-HIFU-heated locations in phantoms. Signal increase was also observed in vivo after iLTSL injection and after each 10-min heating (41°C), with greatest increase in the heated tumour region.

Correspondence: Matthew R. Dreher, Staff Scientist, Clinical Center, National Institutes of Health, Radiology and Imaging Sciences, Room 2N212, Building 10, MSC 1182, 9000 Rockville Pike, Bethesda, MD 20892, USA, Tel: (301) 402-8427. Fax: (301) 496-9933. dreherm@cc.nih.gov.
†These authors contributed equally.

Declaration of interest

NIH may have intellectual property ion the field. NIH and Philips Healthcare have a cooperative research and development agreement. AP is a salaried employee of Philips Healthcare.

Conclusion—An MR imageable liposome formulation co-loaded with doxorubicin and an MR contrast agent was developed. Stability, imageability, and MR-HIFU monitoring and control of content release suggest that MR-HIFU combined with iLTSL may enable real-time monitoring and spatial control of content release.

Keywords

doxorubicin (Adriamycin); heat targeted drug delivery (nanoparticles; liposomes); high intensity focused ultrasound; MR imaging; imageable temperature sensitive liposomes

Introduction

Conventional anticancer chemotherapeutic agents demonstrate limited specificity for tumour tissue that often results in dose-limiting toxicity and reduced therapeutic efficacy. This scenario necessitates development of drug delivery systems (DDS) that may selectively deliver anticancer drugs to a tumour with less harmful side effects, thus resulting in a larger therapeutic window [1]. Among different DDS, liposomes have a long history of delivering both therapeutic and diagnostic agents resulting in a number of liposomal agents being used in the clinic [1, 2].

Liposomal DDS target a solid tumour either ‘passively’, based on factors such as particle size and surface properties, or ‘actively’, due to a specific affinity, activation or stimulus. An example of passive targeting is selective accumulation of stealth (PEGylated) liposomes in solid tumours by a mechanism known as the enhanced permeability and retention (EPR) effect [3, 4]. This approach has often resulted in 10-fold or greater drug delivery to a tumour over conventional chemotherapy [5]. Active drug delivery can be achieved through incorporation of tumour-specific targeting ligands on the surface of the liposome [6, 7] as well as liposomal components sensitive to various stimuli such as pH [8, 9], electromagnetic radiation [10, 11], enzymes [12, 13] and temperature [14–16].

Liposomal formulations with drug release properties that are triggered by heat are called temperature sensitive liposomes (TSLs) [14]. Incorporation of lysolipids in TSL formulations resulted in rapid release of liposomal contents when heated to mild hyperthermia (>40°C), in addition to a slightly lower maximum release temperature than the classical TSLs [15]. These liposomes, with release properties optimised for mild hyperthermia, are often called low temperature sensitive liposomes (LTSLs). Though material properties and efficacy of LTSLs in preclinical and clinical studies have been extensively studied [15, 17–22], precise spatiotemporal control of drug delivery with LTSL has not yet been achieved because it requires the perfect marriage of an LTSL and a hyperthermia applicator with suitable properties. Microwave, radio-frequency and ultrasound hyperthermia applicators have been used. Of these, focused ultrasound applicators provide the most precise delineation of the heated zone as well as the ability to avoid excess heating of subcutaneous fat and skin that plagues other applicator types [23].

Further improvement in spatiotemporal control of drug delivery with LTSL may now be achieved with the recent advances in MR-guided heating methods, such as MR-guided high intensity focused ultrasound (MR-HIFU). MR-guided heating methods are especially relevant to drug delivery with LTSL since they enable accurate and precise spatial and temporal control of heating [24]. Such systems have been approved by the Food and Drug Administration (FDA) [25] and are undergoing clinical trials [26, 27] with temperature feedback [28]. However, intra- and inter-patient spatial variability in tumour microenvironment, such as vascularity and perfusion, may impact both the heating pattern and delivery of drugs [29, 30]. The optimal delivery of HIFU energy to deployed drugs may

theoretically be adjusted for each individual to accommodate for this spatial variability. Therefore, in addition to temperature, direct imaging of drug delivery (or an appropriate surrogate, such as release of an MR contrast agent from LTSL) may improve real-time control of drug delivery or help guide and localise future interventions (such as local thermal ablation).

Co-loading of drug and MR contrast agent into LTSL may provide an appropriate surrogate for drug delivery measurements. The first liposomes loaded with MRI contrast agents appeared in the literature in the 1980s [31]. These encapsulated high concentrations (670 mM) of hydrophilic contrast agents such as Gd-DTPA. Since then, similar Gd-based contrast agents have been incorporated into the liposome interior compartment [32] as well as conjugated to their membrane [33, 34] or both [35]. Most liposomes with Gd-based contrast agents in their interior compartment have a relaxivity lower than that of free contrast agent (>6-fold lower for some liposomes at 1.5 T [31]), because their liposomal membrane shields contrast agent in the interior compartment from bulk water outside the liposome [36]. Liposomes with contrast agents attached to their surface offer exceptionally high relaxivity (>3-fold higher than free contrast agent at 1.5 T [34]), likely due to high rotational correlation times of surface-bound contrast agents [33]. However, such liposomes with contrast agents only on the surface are not designed to report on drug release and may alter other properties of the liposome.

LTSLs that release contrast agent from their interior have been used to image release *in vivo*. Such liposomes have demonstrated promising correlations of MR imaging with ablation margins [37], drug delivery [38] and therapeutic efficacy [39]. While manganese has been used to report on drug delivery with liposomes [38, 39], gadolinium-based contrast agents are more practically attractive due to their likely greater safety profiles and thus greater acceptance in the clinic. Therefore much of the recent work on MR imageable liposomes involves gadolinium-based contrast agents [40].

Ability to image and control content release from liposomes with MR-HIFU may allow for drug dose painting [38, 39]. In this paradigm, the physician would first prescribe a desired dose and spatial distribution of drug to be delivered and then an image-guided hyperthermia applicator would manipulate heat to achieve the desired drug dose. Our dose painting approach employs MR-HIFU to induce drug and contrast agent release from imageable LTSLs, using both imaging of temperature changes and contrast agent release in real-time to control the HIFU transducer to achieve the desired drug distribution in the target volume. As an initial step in this image-guided dose painting concept, the objectives of this study were to: 1) develop iLTSL, an LTSL co-loaded with an FDA-approved MRI contrast agent (ProHance® Gd-HP-DO3A) and doxorubicin (Dox), 2) characterise release of drug and Gd-HP-DO3A from iLTSL, and 3) investigate the ability of MR-HIFU to induce and monitor iLTSL content release in phantoms and *in vivo*.

Materials and methods

Chemicals

ProHance® (Gd-HP-DO3A = 500 mM) (Bracco Diagnostics, Princeton, NJ) was used as the MR contrast agent. Monostearoyl-2-hydroxy-sn-glycero-3-phosphocholine (MSPC), 1,2-dipalmitoyl-sn-glycero-3-phosphocholine (DPPC), and 1,2-distearoyl-sn-glycero-3-phosphoethanolamine-N-[methoxy (Polyethylene Glycol)2000] (DSPE-PEG_{2000}) were obtained from Genzyme Corporation (Cambridge, MA). Dox was obtained from Bedford laboratory (Bedford, OH). High and low melting point agarose was purchased from Invitrogen (Carlsbad, CA) and ISC BioExpress (Kaysville, UT), respectively. All of the other chemicals were bought from Sigma-Aldrich (St Louis, MO).

Preparation and characterisations of iLTSL liposomes

Liposomes were prepared by hydration of lipid film, followed by extrusion as previously reported [41]. Briefly, lipid components (DPPC, MSPC and DSPE-PEG_{2000}) were dissolved in chloroform at a molar ratio of 85.3: 9.7: 5.0. The solvent was evaporated using a Rotovap system and left overnight in a vacuum desiccator. The resulting lipid film was hydrated by a buffer consisting of 300 mM Gd-HP-DO3A and 100 mM Citrate (520 ± 12 mOsm [501–533 mOsm], pH 4.0) at 60°C for 15 min to yield a final lipid concentration of 50 mg/mL. Liposomes were obtained by extruding the mixture five times with a LIPEX™ extruder (Northern Lipids, Burnaby, BC) at 55°C through two stacked Nuclepore® polycarbonate membrane filters (Whatman PLC, Maidstone, Kent, UK) with a pore size of 100 nm.

Encapsulation of Dox into the extruded liposomes was carried out using a pH-gradient loading protocol as described by Mayer et al. [42] with a slight modification: exterior pH of the extruded liposomes was adjusted to 7.4 with sodium carbonate solution (500 mM) creating a pH gradient (acidic inside LTSL). The liposomes were incubated with Dox (Dox:lipid weight ratio of 5: 100) at 37°C for 1 h. Unencapsulated Gd-HP-DO3A and Dox were removed by passing the liposome through a Sephadex-G50 (fine) spin column and the resulting liposomes were stored at 4°C until further use.

Particle size of liposomes was determined by dynamic light scattering (Zetasizer Nano-ZS, Malvern Instruments, Westborough, MA) and reported as the mean Z-averaged diameter, and polydispersity index from a cumulants analysis of three measurements. The concentration of liposome-entrapped Dox was determined using a UV-Vis spectrophotometer (PerkinElmer, Waltham, MA) as previously reported [43].

Dox release

Release of encapsulated Dox from iLTSL as a function of time (up to 15 min) and temperature (25°, and 37°–41.3°C) was assessed by measuring de-quenching of Dox fluorescence as Dox was released from a liposome. Two instruments were used to measure Dox fluorescence in release assays, as necessitated by experimental design. In experiments with high temporal resolution (ThermoScan and Dox release kinetics measurements), fluorescence was measured with a Cary Eclipse spectro-fluorimeter equipped with an Eclipse multicell Peltier temperature controller, and Eclipse Kinetic and ThermoScan Software (Varian, Palo Alto, CA) at excitation and emission wavelengths of 498 and 593 nm, respectively. In experiments where Dox and Gd-HP-DO3A release were both quantified, a Victor II plate reader was used (ex/em = 490/572 nm, Perkin Elmer). Dox release was quantified in three different release assays:

1. *ThermoScan release assay:* In these experiments, Dox release was assessed as a function of both temperature and time. iLTSL stock solution was added to 2 mL of either 10 mM HEPES (pH 7.4, 140 mM NaCl, 280 mOsm) or human plasma (collected with apheresis, whole blood treated with 1: 12 ACD (anticoagulant citrate dextrose solution A)) in a quartz cuvette. The volumes of stock liposome solution added were 8 and 30 μL in experiments for release in HEPES and plasma, respectively. The cuvette was then heated at a rate of 1°C/min from 20°C to 55°C while stirring. Fluorescence readings were taken every 30 s. Another cuvette holder in the Peltier unit was used to monitor temperature. Differences in temperature among the three cuvette holders were less than 0.1°C (data not shown). Data are presented as mean fluorescence intensity ($n = 3$).
2. *Dox kinetic release assay:* These experiments were designed to measure Dox release as a function of time at a constant temperature. The same volumes as above were used, but in this instance, buffer or plasma was first equilibrated to the desired

temperature (25°, 37°–41.3°C). The temperature was maintained and fluorescence intensity was measured every 7 s for 15 min while the sample was stirred. Percentage release was calculated by assuming 100% release with Triton® X-100 and 0% release at 25°C. In HEPES, addition of Triton® X-100 resulted in a decrease (6.7 ± 0.3%, $n = 6$) of Dox fluorescence intensity from the maximum obtained by heating at and above 41°C, and therefore the level of fluorescence used as 100% release was increased proportionately for all release assays of this type in HEPES. In plasma, addition of Triton® X-100 results in an increase of Dox fluorescence of 25.3% (same concentrations of Dox and Triton® X-100 as in the release study). The fluorescence intensity at 100% release (with Triton® X-100) was therefore adjusted proportionately. Data are presented as mean percentage release of three samples ($n = 3$).

3. *Simultaneous Dox and Gd-HP-DO3A release assay:* HEPES buffer (14 mL) or human plasma (7 mL) were allowed to equilibrate in a round-bottomed flask (at 37°, 40°, or 41.3°C). Liposome stock solution was added (1 mL added to HEPES and 0.5 mL to plasma), while mixing with a magnetic stir bar. Aliquots (0.25 mL in HEPES release assay and 0.2 mL in plasma release assay) were withdrawn at predetermined time points. To capture the instantaneous release at each time point, each aliquot was added to 0.75 mL of cooled HEPES buffer or 0.4 mL human plasma on ice. Samples were kept on ice, and longitudinal relaxation rate ($R_1 = 1/T_1$) was measured immediately upon removal from ice to avoid any possible release that may occur at room temperature. During the measurement, temperature increased from 1° to 14°C, but the timing was consistent resulting in reproducible R_1 measurements. After dilution (1: 9 in HEPES, 1: 5 in plasma), fluorescence intensity was measured. For release in HEPES, three replicate wells of a 96-well plate were analysed to determine Dox fluorescence at each time point, whereas 1 well was used for each time point in plasma release assay. Three separate experiments were performed at each temperature, for both HEPES and plasma release ($n = 3$).

Gd-HP-DO3A release

Release of Gd-HP-DO3A was quantified using three methods: 1) measurement of R_1 at 0.5 T before size exclusion chromatography, 2) use of a calibrated relationship between R_1 and contrast agent concentration after size exclusion chromatography and 3) measurements of gadolinium concentration using inductively coupled plasma-atomic emission spectroscopy (ICP-AES).

Samples obtained during the simultaneous Dox and Gd-HP-DO3A release assay (see Dox release above) were used without dilution in the case of plasma release assays. For release measurements in HEPES, samples were further diluted using HEPES to a total volume of 1mL and kept on ice until further analysis. R_1 was measured using a custom-designed variable field T_1 and T_2 analyser (Southwest Research Institute, San Antonio, TX) as previously reported [44]. To approximate R_1 at 100% release, Triton® X-100 (33 μL of 10% w/w in HEPES and 23 μL of 25% w/w in plasma release assays) was added to one sample. This concluded quantification using method 1 for both HEPES and plasma. It is important to note that addition of Triton® X-100 (highest concentration tested and used was 3.5 vol% of 25% Triton® X-100) has no detectable effect on R_1 in either HEPES or plasma.

In HEPES, release was also quantified using methods 2 and 3. Samples were passed through Sephadex-G50 (fine) spin columns twice to remove released contents. Triton® X-100 (33 μL of 10% w/w in HEPES) was added to each sample and R_1 was once again measured using the same procedure. In order to convert the R_1 reading to Gd-HP-DO3A

concentration, a calibration curve was constructed relating R_1 to Gd-HP-DO3A concentration. The same samples whose R_1 was measured above were then analysed for gadolinium and phosphorus content using ICP-AES (Perkin-Elmer Plasma 40), operated at the wavelengths of 342 and 213 nm for gadolinium and phosphorus detection, respectively [45]. These measurements were reported as molar concentrations of Gd-HP-DO3A and as weight percent of Dox and gadolinium with respect to lipid, where the lipid concentration was based on the phosphorus concentration.

Analysis of liposome release kinetics

Temperature of maximum release rate (TMRR) of iLTSL was measured as the maximum of the derivative of the fluorescence–temperature curve obtained in the ThermoScan release assay. In all other assays of release, percentage release of Dox was calculated at time t using the equation given below.

$$\%\,\text{Release}_t = 100\% \cdot \frac{a-b}{c-d} \tag{1}$$

The meaning of the variables in the above equation differs in the three methods used for release measurements of Dox and the three methods of Gd-HP-DO3A release measurements. In the Dox release assays, a represents the fluorescence intensity at time t; b and d are equal to the fluorescence intensity at 25°C and c is the intensity after 100% release.

For the three methods used to measure release of Gd-HP-DO3A, percentage of release was calculated using the following values for the variables in Equation 1. In R_1 measurements before size exclusion chromatography (method 1), a represents R_1 at time t; b and d are values of R_1 at time = 0 s and c is R_1 after the addition of Triton® X-100. In measurement of Gd-HP-DO3A contained inside LTSL after size exclusion chromatography based on R_1 (method 2) and ICP-AES measurements (method 3), a and c represent Gd-HP-DO3A at time = 0 s, while b is Gd-HP-DO3A contained in the internal compartment of the liposome at time t, and d is Gd-HP-DO3A in a sample identical to a and c, but one that was treated with Triton® X-100 before being passed through the columns (Gd-HP-DO3A removed by column). Thus, Equation 1 was modified for methods 2 and 3 to account for the fact that Gd-HP-DO3A released during the assay would be removed by the spin columns.

A least-squares fit of Equation 2 to release curves for Dox and Gd-HP-DO3A (percentage release versus time) was used to calculate the release rate constant k. The first 10 min of data following initiation of release were used in the fit. In this equation, the fit constant Max indicates the maximum percentage release and t represents time in min.

$$\%\text{Release}_t = Max(1-e^{-kt}) \tag{2}$$

Release rate constant reported herein refers to the fitted value of k. Values of percentage release at 15 s and Time to 50% release were interpolated from the fit. Consequently, Time to 50% release could not be measured at the lower temperatures where this level of release was not reached during the assay. Absolute average difference in percentage release was calculated as the average of differences between all of the time points in two release assays, for 10 min following initiation of release. Max was constrained to be greater than 0, and is referred to as Release at 10 min.

Liposome stability

Liposome stability was investigated by measuring size and Dox release kinetics (see Dox kinetic release assay above). Liposome size was measured for 7 consecutive days, and Dox release in HEPES buffer was quantified on day 0 and 7 (at 25°, 37°, 40° and 41°C). Day zero was defined as the day that the LTSLs were prepared. Liposomes were stored at 4°C between measurements.

Measurement of relaxivity

Relaxivity of heated and unheated iLTSL, as well as unencapsulated Gd-HP-DO3A was determined using a clinical 1.5 T MR scanner (Philips Medical Systems, Best, Netherlands) in 10 mM HEPES (pH 7.4, 140 mM NaCl, 280 mOsm). Gd-HP-DO3A was released from iLTSL (final concentration = 0.016–2.0 mM Gd-HP-DO3A) by heating above the TMRR using a hot water bath (55°C for 5 min). R_1 of all of the solutions was calculated as previously reported [46] from the fit of signal intensity vs. inversion time in images obtained with an inversion recovery sequence with variable inversion time (TI = 50, 75, 100, 150, 300, 450, 600, 900, 1050 ms). Relaxivity was obtained as the slope of R_1 versus Gd-HP-DO3A concentration.

Phantom preparation

Tissue mimicking agar-silica phantoms containing iLTSL were prepared using silicon dioxide powder (silicone gel) and agarose powder (2 wt% of each). Each gel-suspended liposome phantom was cast in two stages. First, a larger phantom with a rectangular cavity was made using the higher melting point agarose/silicone gel. After this solidified, the cavity was filled with the low melting point agarose/silicone gel containing iLTSL.

Gel made with higher melting temperature agarose was mixed in de-gassed 280 ± 10 mOsm 0.9% NaCl solution (pH adjusted to 7.4) and heated above 90°C for 30 min while mixing. The gel was slowly cooled at room temperature while mixing to prevent settling of silicone. Upon cooling to 45°C, the gel was poured into a container and set to solidify on ice.

Low melting point agarose gel was used to suspend liposomes and it was prepared in a different fashion than higher melting point agarose gel. After heating above 90°C as above, the agar-silica mixture was allowed to cool to 31°C, at which point iLTSL that was also pre-heated to 31°C was added and mixed with a glass rod to ensure homogeneous distribution of iLTSL in the gel. Once the iLTSL containing gel was well-mixed, it was poured into a cavity within the higher melting point agarose phantom and allowed to solidify. The procedure resulted in an approximate concentration of 1 mM Gd-HP-DO3A in the inner, liposome-containing part of the phantom.

MR-HIFU procedure and imaging of phantoms

Release of iLTSL in phantoms was examined using a Sonalleve MR-HIFU treatment system (Philips Medical Systems, Vantaa, Finland). The system included a clinical 1.5 MRI scanner and an electromechanically positioned ultrasound transducer. The MR system was used to plan the therapy with 3D anatomical imaging and to guide and monitor hyperthermia with thermal imaging during treatment. Heating with MR-HIFU was achieved by focusing an ultrasound beam using a 256-element phased array focused piezoelectric ultrasound transducer immersed in a sealed tank of degassed water, running at 1.2 MHz. A single ~2-mm diameter HIFU focus was steered electronically (by altering the relative phases of transducer elements) [47].

Feedback control of heating relies on the proton resonance frequency shift method [48]. Temperature was raised with constant acoustic power until the mean temperature of the

treatment cell increased above the cut-off temperature (T>42°C). The treatment cell was then allowed to cool for a fixed period of time (30 s). This heat and cool cycle was then repeated to achieve the desired duration of hyperthermia.

Several MR imaging sequences were used to plan the location of heating and to evaluate temperature and contrast agent release. A T_2-weighted, 3D turbo spin-echo (TSE) sequence (TR = 1000 ms, = 80 ms, FA = 90°, TSE train length = 80, 65 slices, FOV = 280 ± 280 cm, 256 ± 160 matrix, NEX = 1) was used to acquire a coronal stack. It was transferred to the HIFU workstation, and used for ultrasound exposure planning. Before and after each heating, a 3D fast field echo (FFE) sequence was used to assess contrast agent release (TR = 10 ms, TE = 3.8 ms, FA = 10°, 44 slices, FOV = 40 ± 40 cm, 256 ± 256 matrix, NEX = 10). To monitor the induced temperature elevation during each heating session, a multi-shot T_2-weighted FFE-EPI sequence was performed every 2.9 s (TR = 39 ms, TE = 19.5 ms, FA =19.5°C, slice thickness = 7 mM, 6 slices, FOV = 40 ± 40 cm, 160 ± 160 matrix, NEX = 1). Each agar-silica gel phantom was positioned on the treatment table, and acoustic coupling was achieved with degassed water. The starting temperature before heating was approximately 13°C.

In vivo imaging of contrast release

All animal experiments were performed under an approved National Institutes of Health Institutional Animal Care and Use Committee protocol. Two New Zealand white rabbits (female, ~3kg) were inoculated with 3×10^6 VX2 cells (150 μL suspension) in the superficial thigh muscle, with ultrasound guidance. Tumour growth was monitored with ultrasound, and the experiments were performed when the tumour was greater than 1 cm in any dimension. Rabbits were anaesthetized with a mixture of ketamine and xylazine (28.6 mg/kg ketamine, 4.8 mg/kg xylazine) and the marginal ear vein was catheterised. Rabbits were transferred to isoflurane anaesthesia, and optical temperature probes were placed in the rectum (used to monitor animal body temperature) and the thigh muscle in the proximity of the tumour (used as input baseline temperature, prior to each sonication). The tumour-bearing limb was partly submerged in degassed deionised water above the HIFU transducer. A high resolution 3D turbo spin echo scan weighted to proton density was used for treatment planning (TR = 1600 ms, TE = 30 ms, slice thickness = 2 mM, 120 slices, FOV = 20 ± 20 cm, 640 ± 640 matrix, NEX = 1). A high resolution T_1-weighted 3D FFE sequence was used to assess signal intensity prior to injection, as well as before and after each sonication (TR = 7 ms, TE = 3 ms, FA = 10°C, slice thickness = 2 mM, 25 slices, FOV = 15 ± 15 cm, 192 ± 192 matrix, NEX = 10). Temperature mapping was performed with a multi-shot T_2-weighted FFE-EPI sequence every 2.5 s (TR = 54 ms, TE = 30 ms, FA = 19°C, 2 slices, FOV = 20 ± 20 cm, 144 ± 144 matrix, NEX = 1). HIFU binary feedback control algorithm was similar to that used in phantom studies (above), with two exceptions: a region of unheated muscle was used to correct for magnetic drift, the temperature in the heated region was maintained between 40° and 41°C.

Statistical analysis

Fitted parameters were compared using the F-test. The values of percentage release were compared using Dunn's multiple comparison. Error reported for interpolated values (time to 50% release and percentage release at 15 s) was calculated as the average of the upper and lower 95% confidence intervals of the fit. Only the first 10 min of release curves were used for fitting. Correlation analyses of temporal particle size and polydispersity index data were performed using the Pearson correlation statistic. All fitting and statistical analyses were performed using GraphPad Prism (version 5.0 for Windows, San Diego, CA). Each curve was considered an independent sample. Results were considered significant with $p < 0.05$, and two-tailed p-values were obtained in all cases. Pairwise comparisons with Dunn's

multiple comparison test were only reported when Kruskal-Wallis showed significant differences between all tested groups to protect against type I error. Values are reported as mean ± SEM.

Results

Characterisation of iLTSL

The Z-average diameter of iLTSL liposomes in four preparations was 98 ± 2 nm and polydispersity index was 0.07 ± 0.02. These liposomes encapsulated 4.97 ± 0.07 wt% Dox based on only Dox and lipid content, or 3.52 ± 0.05 wt% Dox based on Dox, lipid and Gd-HP-DO3A. The amount of Gd-HP-DO3A encapsulated was 18.4 ± 1.2 wt% based on only Gd-HP-DO3A and lipid and 17.6 ± 1.1 wt% based on Dox, lipid and Gd-HP-DO3A. Using a 50 mg/mL lipid preparation and a 300 mM Gd-HP-DO3A hydration buffer resulted in a 59 ± 5 mM Gd-HP-DO3A and 2.14 ± 0.02 mg Dox/mL iLTSL solution.

Dox release

Using fluorescence dequenching, the release of Dox from iLTSL was measured in HEPES buffer as well as in human plasma. Panels A and C of Figure 1 show that Dox fluorescence increased gradually as temperature increased before rapid drug release occurred around TMRR of the liposomal membrane (maximum ion permeability = 41.3°C for similar LTSL [49]). The values of TMRR in these ThermoScan assays were 40.3° ± 0.2°C in HEPES and 38.36 ± 0.17°C in plasma.

When fluorescence was measured at constant temperature in Dox kinetic release assay, Dox release from the LTSL was minimal (<7–20%) at 37–39°C after 15 min in HEPES (Figure 1b). At 40°C there was ~30% released in less than 20 s followed by a more gradual release. Near the TMRR, complete release (>90%) occurred in approximately 7s (by the first measured time point) at 41°C and 41.3°C. Rapid and complete release of Dox also occurred in plasma at these higher temperatures (Figure 1d). The release rate constants in plasma at 39°–41°C were greater than those in buffer (Table I).

Gd-HP-DO3A release

Release of Gd-HP-DO3A was measured with ICP-AES and compared to Dox release in the same sample, as shown in Figure 2a. The difference in percentage release between amounts of Dox and Gd-HP-DO3A was less than 20% for all time points, with the exception of 2 time points at 40°C (at 2 and 3 min, Figure 2a). Differences in the magnitude of Dox and Gd-HP-DO3A percentage release were not significant (p>0.05, Dunn's multiple comparison) over 10 min following initiation of release (mean absolute differences were 0.9 ± 0.2%, 5 ± 1% and 0.5 ± 1% for 37°, 40° and 41.3°C, respectively). This lack of difference in release was especially evident in the first minute of release (Figure 2b). The rates of Dox and Gd-HP-DO3A release are shown in Table II along with other results of the curve fitting. Release of Gd-HP-DO3A was also determined with R_1 measurements (at 0.5 T) before size-exclusion chromatography (Supplementary Figure 1). Agreement between these R_1-based measurements and ICP-AES measurements is shown in Supplementary Figure 2. The temperature measured during simultaneous Dox and Gd-HP-DO3A release assay is shown in Supplementary Figure 3, demonstrating a drop in temperature of 0.5–1°C that recovers approximately 3 min after addition of liposomes. Ratio of gadolinium to phosphate indicated that relative to the lipid concentration, concentration of contrast agent after size exclusion chromatography decreased faster with increasing temperature (Supplementary Figure 4).

In plasma, a comparison of Gd-HP-DO3A and Dox release in the same sample was also performed, with similar results (Figure 2c and d, Table II). Just as with HEPES, all but two

points showed less than 20% difference in percentage release of Dox and Gd-HP-DO3A, and overall, differences in release were not significant over the first 10 min of release ($p>0.05$, Dunn's multiple comparison, Table II). The first minute of release also showed close agreement in the kinetics of Dox and Gd-HP-DO3A release.

Stability of iLTSL

Liposome stability, indicated by lack of temporal dependence of either particle size or polydispersity index ($p>0.05$, Pearson), was relatively constant for one week (95 nm size, polydispersity index = 0.05 at day 0 and 102 nm size, polydispersity index = 0.11 at day 7, $n = 3$). Furthermore, the Dox release rate remained unchanged a week after synthesis and storage of iLTSL at 4°C (Figure 3a). Overall, there was slightly less release on day 7 (mean decrease in release of 0.11 ± 0.14 to 1.83 ± 0.05% over 10 min heating), as indicated by the difference in percentage release (Figure 3b). This difference was significant at 37°C ($p<0.05$, Dunn's multiple comparison test), but not at other temperatures.

Imaging and spatial control of release

Imageability—The ability to image content release from iLTSL was first examined through longitudinal relaxivity measurements. Imaging of a series of dilutions of iLTSL at 1.5 T showed that relaxivity of preheated iLTSL was 4.01 ± 0.01 $mM^{-1}s^{-1}$, which was significantly higher ($p<0.0001$, F-test) than the relaxivity of unheated solutions (1.95 ± 0.05 $mM^{-1}s^{-1}$, Figure 4).

Spatial control of liposomal release

Signal intensity increased approximately 36.4 ± 0.3% in regions of a gel-suspended liposome phantom heated with MR-HIFU above TMRR, compared to the surrounding gel that contained iLTSL but was not heated (Figure 5). The three shapes in Figure 5 reflect pre-programmed trajectories where the HIFU energy was focused demonstrating the ability to yield conformal content release.

Simultaneous imaging of content release and temperature

In a separate experiment, real-time monitoring of temperature and content release from iLTSL was investigated by heating a gel-suspended liposome phantom with MR-HIFU (Figure 6). Phase images were used for MR thermometry and magnitude images were used to measure MR signal intensity. During and after heating, MR-signal intensity increased 36 ± 4% to approximately the same magnitude as the preheated region. The signal intensity of a volume that was unheated remained at its initial level. The temperature fluctuation with HIFU application can be appreciated in Figure 6b, increasing during the heating and decreasing when no power was applied. The duration of each cooling cycle was 30 s, which corresponds to the periods of cooling detected with MR thermometry in Figure 6b.

In vivo feasibility of iLTSL delivery with MR-HIFU

The ability of iLTSL to provide sufficient contrast using MR-HIFU was tested in a rabbit thigh tumour model. Upon injection, signal increased 20–40% in the tumour and remained stable for the 10 min prior to heating. Following each of the four 10-min heating sessions the signal in the heated portion of the tumour increased. After the fourth heating, the signal intensity in the tumour increased 9–22% when compared to immediately after injection. The heated portion of the tumour demonstrated the greatest signal increase (30–60%). Adjacent unheated muscle signal intensity increased 20–25% following injection but remained stable following all of the heating sessions. This study was repeated twice with similar trends.

Discussion

The imageable liposome reported herein incorporated both drug and contrast agent in the interior compartment of liposome, enabling real-time monitoring with MRI of liposomal content release in a heated site. Prior to developing this iLTSL formulation, we identified a set of key design criteria for this liposome, including stability (size and release profiles), imageability (ability to report on content release in MRI), and ease of clinical translation.

Stability

iLTSL stability was assured by optimising the liposome hydrating solution that contains contrast agent and Dox loading buffer. The identity and concentration of both constituents must be properly balanced. Native osmolarity of ProHance® (Gd-HP-DO3A) was 621 mOsm while another common contrast agent, Magnevist™, had an osmolarity of 1960 mOsm for the same 500-mM contrast agent concentration. The lower osmolarity for Gd-HP-DO3A allowed for more contrast agent to be loaded while maintaining stability of the liposome. A 300-mM citrate buffer (≈570 mOsm) is commonly used to actively load Dox into liposomes [50]. In the formulation reported herein, the citrate buffer was reduced to 100 mM to limit osmolarity inside the liposome when combined with 300 mM Gd-HP-DO3A (final osmolarity =~500 mOsm), while at the same time retaining the ability to load 5 wt% Dox. The true osmolarity of the solution inside the liposomes following Dox loading is not known, since Dox forms fibrous structures inside the liposomes due to interactions between Dox, ions and citrate [51]. The osmolarity limit of 500–550 mOsm was empirically determined: loading solutions of greater osmolarity resulted in larger liposomes (>115 nm) that suggested potential instability (data not shown). The choice of 300 mM Gd-HP-DO3A and 100 mM citrate buffer yielded a stable particle size distribution and drug release over one week in storage (Figure 3). Not only the hydration buffer osmolarity, but lipid components may influence stability. A different formulation recently showed similar release properties and improved stability at body temperature [52].

Imageability

iLTSL imageability was optimised by selecting a proper ratio of Gd-HP-DO3A to Dox to provide an MR-signal increase while dosing Dox in a clinically relevant concentration. The balance between imageability (Gd-HP-DO3A) and therapeutic efficacy (Dox), while maintaining stability, is the major consideration for optimisation of a drug plus contrast agent formulation. Although greater amounts of drug have been loaded into imageable liposomes [40], the selection of a relatively low drug:lipid ratio of 5 wt% ensured a [Gd-HP-DO3A] high enough for imaging *in vivo*. This procedure yielded liposomes that would deliver 0.15 mmol/kg of Gd-HP-DO3A at the commonly used 5 mg/kg intravenous dose of Dox-loaded LTSL in mice (approximately 25 mg/m^2 in mice, 2 times lower than human MTD of 50 mg/m^2 [18]), which is sufficient to increase MR signal significantly. Previously reported increase of water exchange across the liposome membrane with temperature increased pre-release R_1, thus attenuating detectability of release with TSLs [40]. iLTSLs demonstrate relaxivity >1 mM^{-1}s^{-1} at room temperature, suggesting that the water exchange rate does impact relaxivity when no release occurred. However, relaxivity at body temperature was not measured and the contents of liposomes investigated herein differ from those previously reported [40]. Therefore, it is unclear to what extent the water exchange rate with iLTSL will decrease the difference in relaxivity before and after release in a physiological setting. Thus the 2-fold increase in relaxivity after contrast agent release from the liposome (Figure 4) reinforced the utility of this formulation in reporting specifically on liposomal content release.

Clinical translation

Clinical translation of iLTSL may be eased by selecting a liposomal formulation with constituents that have a history of clinical use and safety. The MR contrast agent, Gd-HP-DO3A, is currently FDA-approved for imaging abnormal vascularity in the central nervous system and head and neck. Furthermore, Gd-HP-DO3A has demonstrated the lowest incidence of nephrogenic systemic toxicity (NSF) for Gd-based contrast agents [53, 54]. Lastly, the selected lipid components are similar in identity but not in ratio to a commercial formulation, ThermoDox®, (Celsion, Columbia, MD) that has been tested in canine soft tissue sarcomas in a phase I trial [17] and in two phase I trials in human liver tumours with radiofrequency ablation [18–20]. ThermoDox® is currently in a phase III trial with radiofrequency for hepatocellular carcinoma [21] and in a phase I trial in patients with chest wall recurrences of breast cancer [22]. Other FDA-approved liposomal agents use pH gradient loading methods [55]. Although use of FDA-approved and/or clinically used components does not alleviate all safety concerns, these choices may ease clinical translation of the iLTSL imageable liposomal formulation.

Kinetics of release of Dox and Gd-HP-DO3A

While it is preferable to directly image the desired drug for image-guided drug delivery, this is often not possible without chemically modifying the drug. We hope to use co-encapsulated Gd-HP-DO3A as a surrogate of Dox release from a liposome. The release of Dox and Gd-HP-DO3A from the same liposome was evaluated in HEPES buffer and in human plasma without a profound difference for most time points at 37°, 40° and 41°C (Figure 2). Increased relaxivity with heating was also demonstrated (Figure 4), which resulted in greater signal intensity (Figure 5). Taken together, these data suggest that an increase in signal intensity from contrast agent release can be used as a surrogate for drug release from iLTSL.

Release of Dox in plasma was faster than in HEPES buffer at temperatures below TMRR. Tables I and II facilitate a quantitative assessment of the influence of the presence of plasma on release of both Dox and Gd-HP-DO3A. For example, the release rate constant, time to 50% release and release at 15 s provide ways of comparing the rates of drug and contrast release. All of these data point to Dox being released faster in plasma in the intermediate range of temperatures (39–41°C). Furthermore, a comparison of values of TMRR in Table I shows that maximum rate of release of Dox occurs at a lower temperature in plasma. Plasma has been shown to affect liposomal release kinetics [56], and recently it was reported that lysolecithin is lost from LTSL in plasma, and that this phenomenon may play an important role for *in vivo* release kinetics of such liposomes [57]. These observations warrant further investigation into effects of plasma components on TSL release. They also highlight the need to perform release assays of TSLs in plasma to estimate *in vivo* performance.

Release of Gd-HP-DO3A from liposomes was quantified with several methods, and agreement of results from these methods shows that the simplest of the methods could be used in future studies. The main body of this work used ICP-AES, which is a direct measurement of gadolinium. However, this method required removal of released Gd-HP-DO3A from solution using size exclusion chromatography in two steps. Our data suggest that simple R_1-measurements of aliquots collected during the release assay provide an equivalent estimate of percentage release (Supplementary Figure 2). Thus, using this simplified method, the kinetics of Dox and Gd-HP-DO3A were measured in plasma, where separation of released and encapsulated contrast agent would be difficult. This assay (Figure 2) demonstrates that both the contrast agent and Dox are not appreciably released in either HEPES buffer or plasma at 37°C, with the rate and extent of release rising with temperature (Figure 2 and Table II).

A number of methods were used to quantify and describe release of liposomal contents, such as the release rate constant, time to 50% release and release at 15 s. For practical considerations the most important factor is the amount of drug and/or contrast agent released during transit through the treatment volume, as suggested by recent modelling work [58]. Mean transit time in tumours is typically less than 10 s [59], suggesting that drug release must occur in this time window for optimal tumour accumulation. Figure 2 demonstrated no appreciable difference in release of drug and contrast agent on this short time scale, supporting the concept of imaging contrast agent release as a surrogate of drug release. In fact, a 7-s transit time is sufficient for near-maximal content release at 41°C in plasma (Figure 1d). While fast release is important in the heated region, the LTSLs must also stably encapsulate their contents at body temperature. Limited release at 37°C (<15% in 15 min in plasma) ensured that the majority of drug arrives to the heated region stably encapsulated inside iLTSL during a typical hyperthermia treatment (Figure 1d). Further improvement in plasma stability may increase delivery of drug to a heated region.

Drug dose painting using MR-HIFU and iLTSL

The ability of iLTSL to provide sufficient contrast with MR-HIFU was evaluated in a preliminary study that showed MR signal intensity increase after iLTSL injection, followed by further increases after each 10-min hyperthermia treatment (Figure 7). Since Dox and Gd-HP-DO3A release are well correlated, it is our hope that Dox concentration may be related to MR signal changes. However, since Gd-HP-DO3A and Dox have different physicochemical properties, a computational model that takes this into account may be required [58]. Correlation of MR signal intensity and Dox concentration will be the subject of future investigations.

Two *in vivo* studies recently addressed the possibility of drug dose painting with LTSLs co-loaded with an MR contrast agent and Dox [38, 39]. However, the hyperthermia system used in these studies could not quickly adjust temperature distribution in the heated volume. Real-time adjustment of treatment would best be accomplished through dynamic imaging during heating as demonstrated in phantoms (Figure 6). For *in vivo* applications, we believe quantifying drug release on a voxel-by-voxel basis may provide useful information to optimise a treatment.

Recent development and therapeutic clinical use of MR-HIFU may provide a method for using imageable temperature-sensitive liposomes for drug dose painting with higher precision and accuracy than previous hyperthermia applicators (4-mm regions have been reliably heated with temperature feedback [28]). The MR-HIFU system we adopted for mild hyperthermia is currently in clinical trials for ablative treatment of uterine fibroids with MR thermometry feedback [26, 27] and other systems have already been approved by FDA [25].

The MR-HIFU system's ability to dose paint with various shapes, control temperature and monitor liposome release is demonstrated in Figures 5 and 6. The system is able to heat a tumour *in vivo* and cause preferential signal intensity increase in the heated region, presumably due to contrast agent release from iLTSL (Figure 7). However, the MRI sequence used for simultaneous temperature and contrast agent release monitoring (Figure 6) was optimised only for temperature imaging, which resulted in $T_2^{\star}$-weighted images. Thus, there is a clear need for an imaging approach with greater T_1 contrast along with satisfactory temperature feedback for MR-HIFU. Combination of a precise hyperthermia applicator, MR thermometry, T_1-weighted imaging, computational modelling, and imageable LTSLs with suitable properties may realise a dose painting paradigm for treatment of cancer and other diseases. Such spatially tuned targeting of cancer and other locally dominant diseases may provide a novel dimension for drug delivery that can take

advantage of a device specially optimised for drug delivery. Furthermore, knowledge of the location of drug release may address clinical deficiencies by facilitating future treatments.

Conclusion

This work demonstrated preparation and characterisation of a novel MR imageable liposome formulation co-loaded with Dox and an MR contrast agent, Gd-HP-DO3A. The design of the formulation ensured stability during storage and imageability of content release. Monitoring and spatial control of liposomal content release was demonstrated with MR-HIFU in tissue-mimicking phantoms in real time, as well as after heating *in vivo*.

Supplementary Material

Refer to Web version on PubMed Central for supplementary material.

Acknowledgments

This work was supported in part by the Intramural Research Program of the National Institutes of Health, the National Institutes of Health Center for Interventional Oncology, and a grant from the NIH/NCI CA42745-22 and -23.

References

1. Allen TM, Cullis PR. Drug delivery systems: Entering the mainstream. Science. 2004; 303:1818–1822. [PubMed: 15031496]
2. Tilcock C. Delivery of contrast agents for magnetic resonance imaging, computed tomography, nuclear medicine and ultrasound. Adv Drug Deliv Rev. 1999; 37:33–51. [PubMed: 10837725]
3. Maeda H, Seymour LW, Miyamoto Y. Conjugates of anticancer agents and polymers - advantages of macromolecular therapeutics *in vivo*. Bioconjugate Chem. 1992; 3:351–362.
4. Matsumura Y, Maeda H. A new concept for macromolecular therapeutics in cancer-chemotherapy - mechanism of tumori-tropic accumulation of proteins and the antitumor agent SMANCS. Cancer Res. 1986; 46:6387–6392. [PubMed: 2946403]
5. Northfelt DW, Martin FJ, Working P, Volberding PA, Russell J, Newman M, Amantea MA, Kaplan LD. Doxorubicin encapsulated in liposomes containing surface-bound polyethylene glycol: Pharmacokinetics, tumor localization, and safety in patients with AIDS-related Kaposi's sarcoma. J Clin Pharmacol. 1996; 36:55–63. [PubMed: 8932544]
6. Allen TM. Ligand-targeted therapeutics in anticancer therapy. Nat Rev Cancer. 2002; 2:750–763. [PubMed: 12360278]
7. Negussie AH, Miller JL, Reddy G, Drake SK, Wood BJ, Dreher MR. Synthesis and in vitro evaluation of cyclic NGR peptide targeted thermally sensitive liposome. J Control Release. 2010; 2:265–273. [PubMed: 20067811]
8. Simoes S, Moreira JN, Fonseca C, Duzgunes N, de Lima MCP. On the formulation of pH-sensitive long circulation times. Adv Drug Del Rev. 2004; 56:947–965.
9. Lokling KE, Fossheim SL, Klaveness J, Skurtveit R. Biodistribution of pH-responsive liposomes for MRI and a novel approach to improve the pH-responsiveness. J Control Release. 2004; 98:87–95. [PubMed: 15245892]
10. Spratt T, Bondurant B, O'Brien DF. Rapid release of liposomal contents upon photoinitiated destabilization with UV exposure. BBA-Biomembranes. 2003; 1611:35–43. [PubMed: 12659943]
11. Shum P, Kim JM, Thompson DH. Phototriggering of liposomal drug delivery systems. Adv Drug Del Rev. 2001; 53:273–284.
12. Jensen SS, Andresen TL, Davidsen J, Hoyrup P, Shnyder SD, Bibby MC, Gill JH, Jorgensen K. Secretory phospholipase A2 as a tumor-specific trigger for targeted delivery of a novel class of liposomal prodrug anticancer etherlipids. Mol Cancer Ther. 2004; 3:1451–1458. [PubMed: 15542784]

13. Pak CC, Erukulla RK, Ahl PL, Janoff AS, Meers P. Elastase activated liposomal delivery to nucleated cells. BBA-Biomembranes. 1999; 1419:111–126. [PubMed: 10407064]

14. Yatvin MB, Weinstein JN, Dennis WH, Blumenthal R. Design of liposomes for enhanced local release of drugs by hyperthermia. Science. 1978; 202:1290–1293. [PubMed: 364652]

15. Needham D, Anyarambhatla G, Kong G, Dewhirst MW. A new temperature-sensitive liposome for use with mild hyperthermia: Characterization and testing in a human tumor xenograft model. Cancer Res. 2000; 60:1197–1201. [PubMed: 10728674]

16. Lindner LH, Eichhorn ME, Eibl H, Teichert N, Schmitt-Sody M, Issels RD, Dellian M. Novel temperature-sensitive liposomes with prolonged circulation time. Clin Cancer Res. 2004; 10:2168–2178. [PubMed: 15041738]

17. Hauck ML, LaRue SM, Petros WP, Poulson JM, Yu D, Spasojevic I, Pruitt AF, Klein A, Case B, Thrall DE, et al. Phase I trial of doxorubicin-containing low temperature sensitive liposomes in spontaneous canine tumors. Clin Cancer Res. 2006; 12:4004–4010. [PubMed: 16818699]

18. Poon RT, Borys N. Lyso-thermosensitive liposomal doxorubicin: A novel approach to enhance efficacy of thermal ablation of liver cancer. Expert Opin Pharmacother. 2009; 10:333–343. [PubMed: 19236203]

19. Celsion. [accessed 14 February 2010] A phase I dose escalation tolerability study of ThermoDox™ (thermally sensitive liposomal doxorubicin) in combination with radiofrequency ablation (RFA) of primary and metastatic tumors of the liver. Available from: http://www.clinicaltrials.gov/ct2/show/NCT00441376

20. National Cancer Institute. [accessed 14 February 2010] A phase I dose escalation study of heat activated liposome delivery of doxorubicin and radio-frequency ablation of primary and metastatic tumors of the liver. Available from: http://www.clinicaltrials.gov/ct2/show/NCT00093444

21. Celsion. [accessed 14 February 2010] A phase III, randomized, double-blinded, dummy-controlled study of the efficacy and safety of ThermoDox® (thermally sensitive liposomal doxorubicin) in combination with radiofrequency ablation (RFA) compared to RFA-alone in the treatment of non-resectable hepatocellular carcinoma. Available from: http://www.clinicaltrials.gov/ct2/show/NCT00617981

22. Duke University and National Cancer Institute. [accessed 14 February 2010] A phase I, dose escalation and pharmacokinetics study of temperature sensitive liposome encapsulated doxorubicin(ThermoDox™) and hyperthermia in patients with local-regionally recurrent breast cancer. Available from: http://www.clinicaltrials.gov/ct2/show/NCT00346229

23. Hand, JW. Principles of ultrasound used for generating localized hyperthermia. In: Field, SB.; Hand, JW., editors. An Introduction to the Practical Aspects of Clinical Hyperthermia. London: Taylor & Francis; 1990. p. 371-422.

24. McDannold N, Hynynen K, Wolf D, Wolf G, Jolesz F. MRI evaluation of thermal ablation of tumors with focused ultrasound. J Magn Reson Imaging. 1998; 8:91–100. [PubMed: 9500266]

25. Stewart EA, Rabinovici J, Tempany CM, Inbar Y, Regan L, Gostout B, Hesley G, Kim HS, Hengst S, Gedroyc WM. Clinical outcomes of focused ultrasound surgery for the treatment of uterine fibroids. Fertil Steril. 2006; 85:22–29. [PubMed: 16412721]

26. Phillips Healthcare and NICHD. [accessed 20 April 2010] Pilot study of MRI-guided high intensity focused ultrasound ablation of uterine fibroids. Available from: http://www.clinicaltrials.gov/ct2/show/NCT00837161

27. Phillips Healthcare and Phillips Medical Systems. [accessed 20 April 2010] Clinical trial protocol for therapeutic MRI-guided high intensity focused ultrasound ablation of uterine fibroids. Available from: http://www.clinicaltrials.gov/ct2/show/NCT00897897

28. Enholm JK, Kohler MO, Quesson B, Mougenot C, Moonen CT, Sokka SD. Improved volumetric MR-HIFU ablation by robust binary feedback control. IEEE Trans Biomed Eng. 2010; 57:103–113. [PubMed: 19846364]

29. Schramm W, Yang D, Haemmerich D. Contribution of direct heating, thermal conduction and perfusion during radio-frequency and microwave ablation. Conf Proc IEEE Eng Med Biol Soc. 2006; 1:5013–5016. [PubMed: 17946669]

30. Freccero C, Holmlund F, Bornmyr S, Castenfors J, Johansson AM, Sundkvist G, Svensson H, Wollmer P. Laser Doppler perfusion monitoring of skin blood flow at different depths in finger and arm upon local heating. Microvasc Res. 2003; 66:183–189. [PubMed: 14609523]
31. Tilcock C, Unger E, Cullis P, MacDougall P. Liposomal Gd-DTPA: Preparation and characterization of relaxivity. Radiology. 1989; 171:77–80. [PubMed: 2928549]
32. Ghaghada K, Hawley C, Kawaji K, Annapragada A, Mukundan S. T1 relaxivity of core-encapsulated gadolinium liposomal contrast agents - Effect of liposome size and internal gadolinium concentration. Acad Radiol. 2008; 15:1259–1263. [PubMed: 18790397]
33. Mulder WJM, Strijkers GJ, Griffioen AW, van Bloois L, Molema G, Storm G, Koning GA, Nicolay K. A liposomal system for contrast-enhanced magnetic resonance imaging of molecular targets. Bioconjugate Chem. 2004; 15:799–806.
34. Laurent S, Elst LV, Thirifays C, Muller RN. Paramagnetic liposomes: Inner versus outer membrane relaxivity of DPPC liposomes incorporating lipophilic gadolinium complexes. Langmuir. 2008; 24:4347–4351. [PubMed: 18338913]
35. Ghaghada KB, Ravoori M, Sabapathy D, Bankson J, Kundra V, Annapragada A. New Dual Mode Gadolinium Nanoparticle Contrast Agent for Magnetic Resonance Imaging. PLoS ONE. 2009; 4(10):e7628.10.1371/journal.pone.0007628 [PubMed: 19893616]
36. Koenig SH, Ahkong QF, Brown RD, Lafleur M, Spiller M, Unger E, Tilcock C. Permeability of liposomal membranes to water - Results from the magnetic-field dependence of T1 of solvent protons in suspensions of vesicles with entrapped paramagnetic-ions. Magn Reson Med. 1992; 23:275–286. [PubMed: 1549042]
37. Frich L, Bjornerud A, Fossheim S, Tillung T, Gladhaug I. Experimental application of thermosensitive paramagnetic liposomes for monitoring magnetic resonance imaging guided thermal ablation. Magn Reson Med. 2004; 52:1302–1309. [PubMed: 15562487]
38. Viglianti BL, Abraham SA, Michelich CR, Yarmolenko PS, MacFall JR, Bally MB, Dewhirst MW. *In vivo* monitoring of tissue pharmacokinetics of liposome/drug using MRI: Illustration of targeted delivery. Magn Reson Med. 2004; 51:1153–1162. [PubMed: 15170835]
39. Ponce AM, Viglianti BL, Yu D, Yarmolenko PS, Michelich CR, Woo J, Bally MB, Dewhirst MW. Magnetic resonance imaging of temperature-sensitive liposome release: Drug dose painting and antitumor effects. J Natl Cancer Inst. 2007; 99:53–63. [PubMed: 17202113]
40. de Smet M, Langereis S, den Bosch SV, Grull H. Temperature-sensitive liposomes for doxorubicin delivery under MRI guidance. J Control Release. 2009; 1:120–127. [PubMed: 19969035]
41. Mayer LD, Bally MB, Hope MJ, Cullis PR. Uptake of antineoplastic agents into large unilamellar vesicles in response to a membrane potential. Biochim Biophys Acta. 1985; 816:294–302. [PubMed: 3839135]
42. Mayer LD, Bally MB, Cullis PR. Uptake of adriamycin into large unilamellar vesicles in response to a pH gradient. Biochim Biophys Acta. 1986; 857:123–126. [PubMed: 3964703]
43. Fenske, DB.; Maurer, N.; Cullis, P. Liposomes. 2. Oxford: Oxford University Press; 2003.
44. Bryant LH, Brechbiel MW, Wu CC, Bulte JWM, Herynek V, Frank JA. Synthesis and relaxometry of high-generation (G = 5, 7, 9, and 10) PAMAM dendrimer-DOTA-gadolinium chelates. J Magn Reson Imaging. 1999; 9:348–352. [PubMed: 10077036]
45. Molinelli AR, Madden MC, McGee JK, Stonehuerner JG, Ghio AJ. Effect of metal removal on the toxicity of airborne particulate matter from the Utah Valley. Inhal Toxicol. 2002; 14:1069–1086. [PubMed: 12396411]
46. Bluml S, Schad LR, Stepanow B, Lorenz WJ. Spin-lattice relaxation-time measurement by means of a turboflash technique. Magn Reson Med. 1993; 30:289–295. [PubMed: 8412599]
47. Salomir R, Palussiere J, Vimeux FC, de Zwart JA, Quesson B, Gauchet M, Lelong P, Pergrale J, Grenier N, Moonen CT. Local hyperthermia with MR-guided focused ultrasound: Spiral trajectory of the focal point optimized for temperature uniformity in the target region. J Magn Reson Imaging. 2000; 12:571–583. [PubMed: 11042639]
48. Hindman JC. Proton resonance shift of water in the gas and liquid states. J Chem Phys. 1966; 44:4582–4592.

49. Mills JK, Needham D. Lysolipid incorporation in dipalmitoylphosphatidylcholine bilayer membranes enhances the ion permeability and drug release rates at the membrane phase transition. Biochim Biophys Acta. 2005; 1716:77–96. [PubMed: 16216216]
50. Madden TD, Harrigan PR, Tai LC, Bally MB, Mayer LD, Redelmeier TE, Loughrey HC, Tilcock CP, Reinish LW, Cullis PR. The accumulation of drugs within large unilamellar vesicles exhibiting a proton gradient: A survey. Chem Phys Lipids. 1990; 53:37–46. [PubMed: 1972352]
51. Li X, Hirsh DJ, Cabral-Lilly D, Zirkel A, Gruner SM, Janoff AS, Perkins WR. Doxorubicin physical state in solution and inside liposomes loaded via a pH gradient. Biochim Biophys Acta. 1998; 1415:23–40. [PubMed: 9858673]
52. Hossann M, Wiggenhorn M, Schwerdt A, Wachholz K, Teichert N, Eibl H, Issels RD, Lindner LH. *In vitro* stability and content release properties of phosphatidylglyceroglycerol containing thermosensitive liposomes. Biochim Biophys Acta. 2007; 1768:2491–2499. [PubMed: 17618599]
53. Port M, Idee JM, Medina C, Robic C, Sabatou M, Corot C. Efficiency, thermodynamic and kinetic stability of marketed gadolinium chelates and their possible clinical consequences: A critical review. Biometals. 2008; 21:469–490. [PubMed: 18344005]
54. Kanal E, Barkovich AJ, Bell C, Borgstede JP, Bradley WG, Froelich JW, Gilk T, Gimbel JR, Gosbee J, Kuhni-Kaminski E, et al. Safety ACRBRPM. ACR Guidance document for safe MR practices: 2007. Am J Roentgenol. 2007; 188:1447–1474. [PubMed: 17515363]
55. Barenholz Y. Relevancy of drug loading to liposomal formulation therapeutic efficacy. J Liposome Res. 2003; 13:1–8. [PubMed: 12725720]
56. Allen TM, Cleland LG. Serum-induced leakage of liposome contents. Biochim Biophys Acta. 1980; 597:418–426. [PubMed: 7370258]
57. Banno B, Ickenstein LM, Chiu GNC, Bally MB, Thewalt J, Brief E, Wasan EK. The functional roles of poly(ethylene glycol)-lipid and lysolipid in the drug retention and release from lysolipid-containing thermosensitive liposomes *in vitro* and *in vivo*. J Pharm Sci. 2010; 99:2295–2308. [PubMed: 19902527]
58. Gasselhuber A, Dreher MR, Negussie A, Wood BJ, Rattay F, Haemmerich D. Mathematical spatio-temporal model of drug delivery from low temperature sensitive liposomes during radiofrequency tumour ablation. Int J Hyperthermia. 2010; 26(5):499–513. [PubMed: 20377363]
59. Sahani DV, Kalva SP, Hamberg LM, Hahn PF, Willett CG, Saini S, Mueller PR, Lee TY. Assessing tumor perfusion and treatment response in rectal cancer with multisection CT: Initial observations. Radiology. 2005; 234:785–792. [PubMed: 15734934]

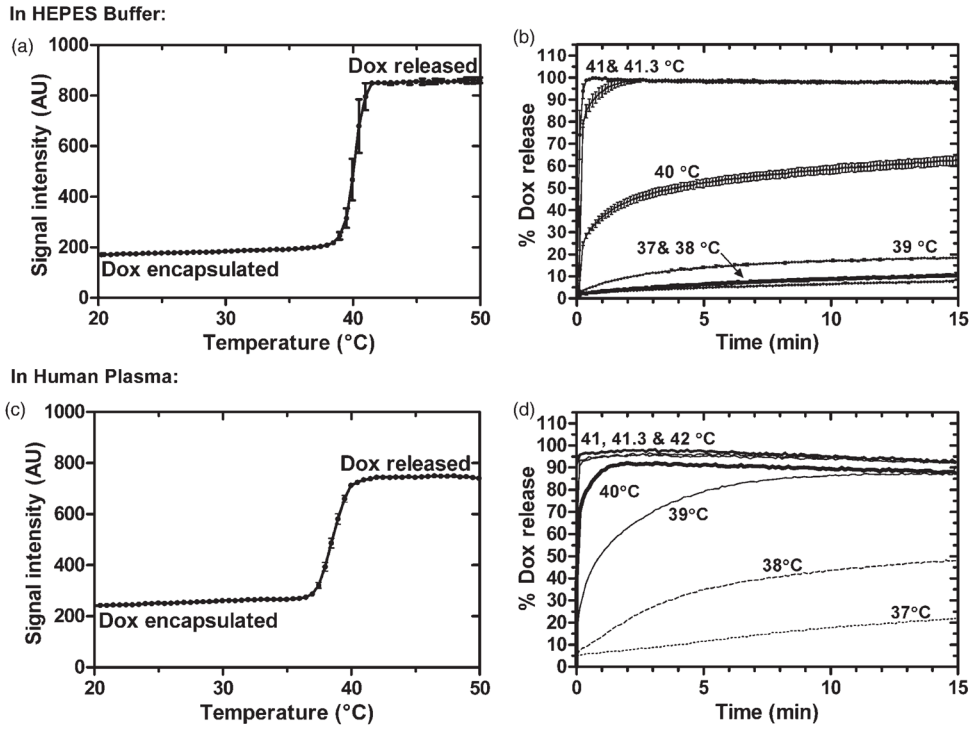

Figure 1.

Release from iLTSL in HEPES buffer and human plasma. (a) Release of Dox as a function of temperature is shown as the sample is heated from 20 to 55°C at 1°C/min. Note that in this graph, the influence of temperature and time are coupled. (b) Dox release as a function of time at a constant temperature. Percent release is calculated by assuming 100% release with TritonÒ X-100 and 0% release at 25°C. (c) and (d) show the same data for release in human plasma.

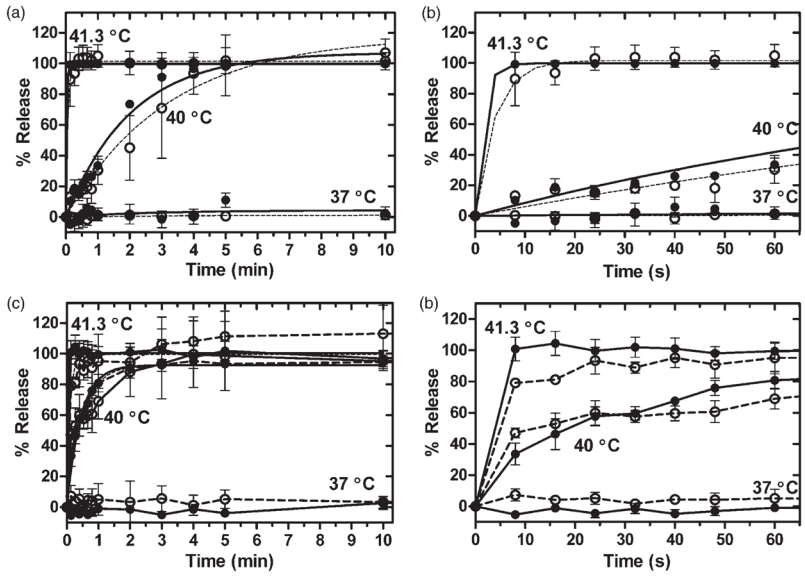

Figure 2.

Release of Dox and Gd-HP-DO3A from iLTSL. Release in HEPES: (a) Percent release vs. time and fitted curves for Dox (○- -) and Gd-HP-DO3A ((●–)over 10 min. (b) The first minute of release. Percent release values were not significantly different between Dox and Gd-HP-DO3A over 10 minutes (p>0.05, Dunn's multiple comparison). Release in plasma: (c) Percent release vs. time for Dox and Gd-HP-DO3A over 10 min. d) The first minute of release. Percent release values were not significantly different between Dox and Gd-HP-DO3A in either HEPES or plasma (p>0.05, Dunn's multiple comparison). Each point represents the mean of 3 experiments ± SEM.

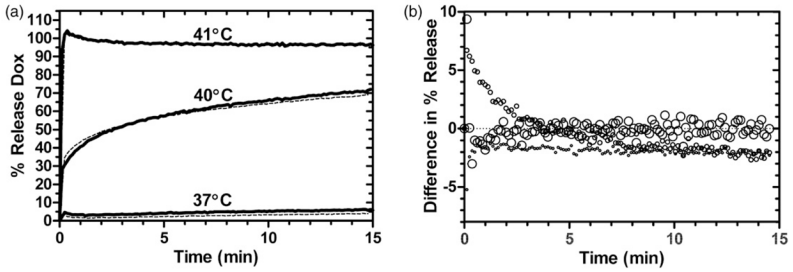

Figure 3.

Stability of Gd-LTSL-DOX. a) Release of doxorubicin immediately (dashed line) and 7 days after synthesis (solid line) of Gd-LTSL-DOX at 37, 40 and 41°C in HEPES buffer. b) Point-by-point difference between release curves at 37, 40 and 41°C obtained 1 week apart (%release at day 0 – %release at day 7). Symbol size indicates temperature: 37°C is smallest (○- -) and 41°C is largest (●–).

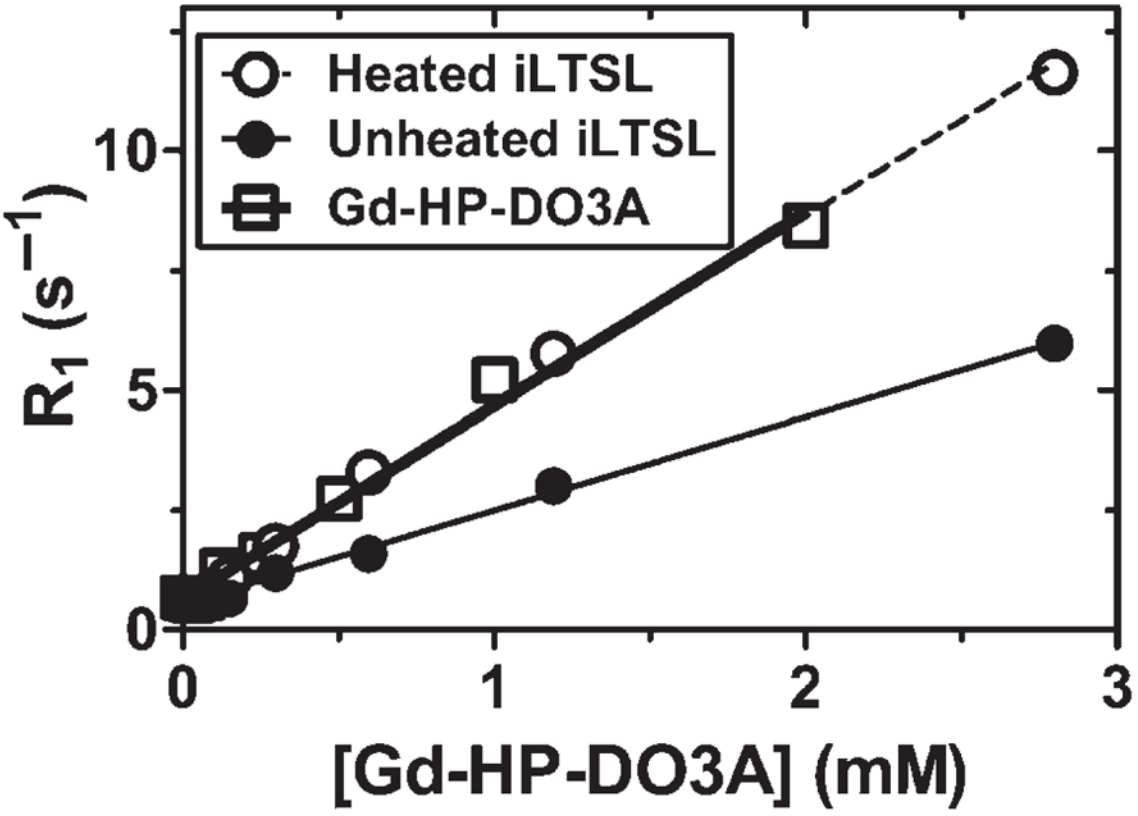

Figure 4.
Relaxation rate (R1) versus concentration of Gd-HP-DO3A at 1.5T. Gd-LTSL-DOX solutions were heated in a water bath (55°C for 5 min) to release Gd-HP-DO3A and the drug. The resulting relaxivity (slope) values for heated and unheated iLTSL were 4.01 ± 0.01 and 1.95 ± 0.05 mM-1s-1, respectively, and were significantly different ($p < 0.0001$, F test). Relaxivity of Gd-HP-DO3A (4.05 ± 0.14 mM-1s-1) was not significantly different from that of heated iLTSL ($p = 0.85$, F test). R2>0.992 for all fitted data.

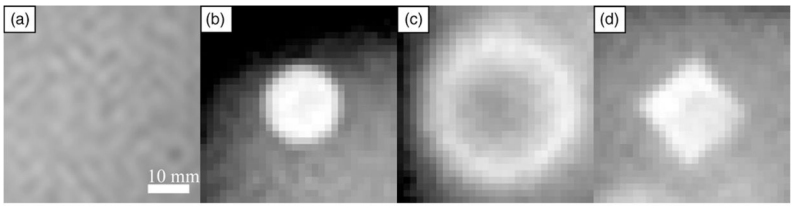

Figure 5.
Location of release of iLTSL contents can be controlled and visualized with MR-HIFU. iLTSL suspended in 2% agar-silica demonstrated baseline intensity (a) until heated above the Tm of the liposome with MR-HIFU (b – d). The bright shapes result from different sizes and shapes of regions that were heated with MR-HIFU.

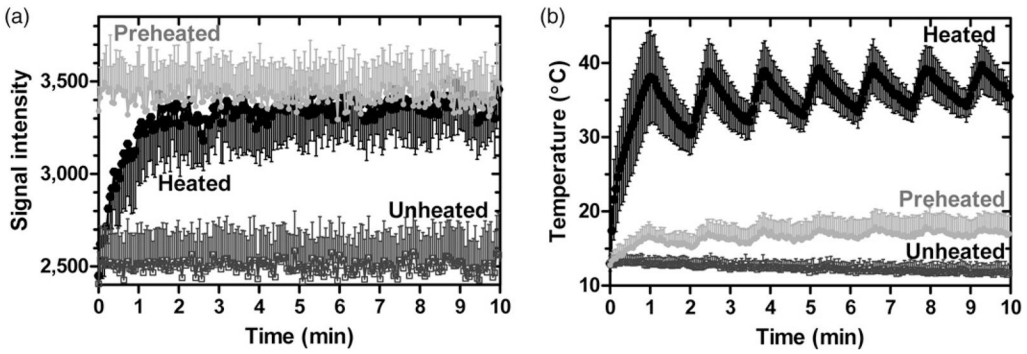

Figure 6.

MR signal intensity during heating with MR-HIFU of a silica-agarose gel phantom containing iLTSL. a) MR signal intensity in heated, unheated, as well as preheated regions. b) Temperature in the same regions, as measured with MR thermometry. Signal intensity of the region where the MR-HIFU energy is focused increased most likely due to Gd-HP-DO3A release. The signal intensity in a region that has been previously heated did not change drastically, but remained high relative to unheated regions. An unheated region demonstrated stable and relatively low signal intensity. Regions of interest contained 20–45 voxels. Mean signal/temperature ± SEM is shown.

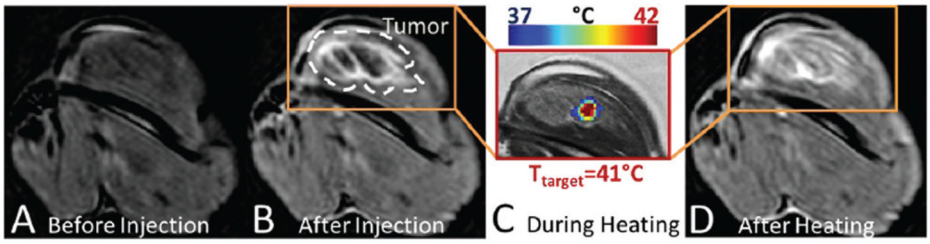

Figure 7.
MR signal intensity before and after iLTSL injection and heating with MR-HIFU. Signal intensity a) before iLTSL injection and b) after iLTSL injection. c) Example of temperature map during heating, overlaid on signal intensity obtained with a treatment planning proton density weighted scan. d) Signal intensity after four 10-minute heating sessions. Note that (a), (b) and (d) depict T1-weighted images whereas (c) shows a proton density weighted image.

Table I

Summary of both kinetic and ThermoScan Dox release assays in HEPES buffer and human plasma.

		37°C	38°C	39°C	40°C	41°C	41.3°C
HEPES	Release rate constant (min^{-1})	0.44 ± 0.03★★	0.3 ± 0.02	0.427 ± 0.011★★	1.05 ± 0.04★★	4.5 ± 0.1★★	11.6 ± 0.3★★
	Time to 50% release (s)	N/A	N/A	N/A	150 ± 10	9.4 ± 0.6	3.7 ± 0.2
	Release at 15s (%)	0.65 ± 0.06	0.63 ± 0.08	1.73 ± 0.05	11.4 ± 0.6	57 ± 3	59 ± 4
	Release at 10 min (%)	5.90 ± 0.11★★	8.7 ± 0.2★★	16.54 ± 0.12★★	54.0 ± 0.4★★	98.4 ± 0.2★★	98.42 ± 0.13★★
	R^2	0.6409	0.7677	0.9506	0.8367	0.9319	0.9709
	TMRR (°C)			40.3 ± 0.2			
Plasma	Release rate constant (min^{-1})	0.224 ± 0.013★★	0.304 ± 0.004	0.76 ± 0.02★★	4.74 ± 0.14★★	8.9 ± 0.4★★	8.5 ± 0.4★★
	Time to 50% release (s)	N/A	N/A	68 ± 3	0.073 ± 0.012	0.039 ± 0.004	0.043 ± 0.005
	Release at 15s (%)	5.0 ± 0.2	7.0 ± 0.3	28.3 ± 1.4	89.8 ± 0.5	94.8 ± 0.4	95.4 ± 0.4
	Release at 10 min (%)	18.2 ± 0.5★★	44.5 ± 0.2★★	82.6 ± 0.4★★	90.6 ± 0.2★★	95.0 ± 0.2★★	95.6 ± 0.2★★
	R^2	0.8548	0.9895	0.9332	0.9439	0.9349	0.9071
	TMRR (°C)			38.36 ± 0.17			
	Absolute average difference (%)	6.6 ± 0.3	24.7 ± 1.0★★	59.2 ± 1.5★★	39.1 ± 0.83★★	2.2 ± 0.5★★	3.1 ± 0.2★★

Fitted values ('Release rate constant' and 'Release at 10min') are reported with their standard errors and values interpolated from the fits ('Time to 50% release', 'Release at 15s') are reported with average 95% confidence intervals. Temperature of maximum release rate (TMRR) was the maximum of the derivative of the fluorescence-temperature curve obtained in the ThermoScan release assay. Absolute average difference is the difference in average release between HEPES and plasma over 10 min. Significance is shown for HEPES vs. plasma comparisons:

★ *and* ★★ indicate significant differences with $p < 0.05$ and $p < 0.01$, respectively.

Table II

Summary of Gd-HP-DO3A and Dox release from Gd-LTSL-DOX in HEPES and Plasma.

		37°C	40°C	41.3°C
In HEPES				
Dox	Release rate constant (min^{-1})	0.3 ± 0.7	0.31 ± 0.05★★	15 ± 2★★
	Release at 10 min (%)	1.2 ± 1.5	118 ± 9	101.6 ± 1.3
	Time to 50% release (s)	N/A	106 ± 19	2.7 ± 0.8
	Release at 15s (%)	0.1 ± 0.2	9 ± 2	99 ± 3
	R^2	0.04916	0.8885	0.9357
Gd-HP-DO3A	Release rate constant (min^{-1})	0.4 ± 1.0	0.49 ± 0.04★★	38 ± 2★★
	Release at 10 min (%)	4 ± 5	107 ± 3	99.82 ± 0.04
	Time to 50% release (s)	N/A	76 ± 8	1.1 ± 0.1
	Release at 15s	0.4 ± 1.2	12.4 ± 1.3	99.81 ± 0.09
	R^2	0.04856	0.9669	0.9999
	Absolute average difference (%)	0.9 ± 0.2	5 ± 1	0.5 ± 1
In plasma				
Dox	Release rate constant (min^{-1})	Not converged	2.1 ± 0.3	9 ± 2
	Release at 10 min (%)	N/A	92 ± 4	100 ± 3
	Time to 50% release (s)	N/A	23 ± 6	4 ± 2
	Release at 15s	N/A	37 ± 7	90 ± 9
	R^2	N/A	0.7182	0.7955
Gd-HP-DO3A	Release rate constant (min^{-1})	Not converged	2.3 ± 0.2	Not converged
	Release at 10 min (%)	N/A	92 ± 2	N/A
	Time to 50% release (s)	N/A	21 ± 3	N/A
	Release at 15s	N/A	40 ± 4	N/A
	R^2	N/A	0.9258	N/A
	Absolute average difference (%)	6.2 ± 1.2	5.6 ± 1.6	10 ± 2

Release characteristics obtained from the simultaneous Dox and Gd-HP-DO3A release assay (Figure 2). Fitted values (‘Release rate constant’, ‘Release at 10 min’) are reported with their standard errors and values interpolated from the fits (‘Time to 50% release’, ‘Release at 15s’) are reported with average 95% confidence intervals. Absolute average difference is the difference in average release between Dox and Gd-HP-DO3A over 10 min. Statistical significance for Dox vs. Gd-HP-DO3A comparisons is shown:

★ *and* ★★ indicate significant differences with $p < 0.05$ and $p < 0.01$, respectively.